

Heterologous Expression of *sahH* Reveals That Biofilm Formation Is Autoinducer-2-independent in *Streptococcus sanguinis* but Is Associated with an Intact Activated Methionine Cycle^{*[5]}

Received for publication, May 7, 2012, and in revised form, August 27, 2012. Published, JBC Papers in Press, August 31, 2012, DOI 10.1074/jbc.M112.379230

Sylvio Redanz, Kerstin Standar, Andreas Podbielski, and Bernd Kreikemeyer¹

From the Institute of Medical Microbiology, Virology and Hygiene, Rostock University Hospital, 18057 Rostock, Germany

Background: AI-2 is a by-product of the LuxS-mediated reaction within the activated methionine cycle (AMC).

Results: The biofilm phenotype of a *S. sanguinis luxS* mutant was restored by SahH expression but not by AI-2 supplementation.

Conclusion: The *luxS* mutant biofilm phenotype is not caused by lacking AI-2 but by an AMC defect.

Significance: The SahH bypass is essential for further studies on AI-2 utilizing *luxS* mutants.

Numerous studies have claimed deleterious effects of LuxS mutation on many bacterial phenotypes, including bacterial biofilm formation. Genetic complementation mostly restored the observed mutant phenotypes to WT levels, leading to the postulation that quorum sensing via a family of molecules generically termed autoinducer-2 (AI-2) is essential for many phenotypes. Because LuxS mutation has dual effects, this hypothesis needs to be investigated into the details for each bacterial species. In this study we used *S. sanguinis* SK36 as a model biofilm bacterium and employed physiological characterization and transcriptome approaches on WT and *luxS*-deficient strains, in combination with chemical, *luxS*, and *sahH* complementation experiments. SahH enables a direct conversion of SAH to homocysteine and thereby restores the activated methionine cycle in a *luxS*-negative background without formation of the AI-2 precursor 4,5-dihydroxy-2,3-pentanedione. With this strategy we were able to dissect the individual contribution of LuxS and AI-2 activity in detail. Our data revealed that *S. sanguinis* biofilm formation is independent from AI-2 substance pools and is rather supported by an intact activated methyl cycle. Of 216 differentially transcribed genes in the *luxS* mutant, 209 were restored by complementation with a gene encoding the S-adenosylhomocysteine hydrolase. Only nine genes, mainly involved in natural competence, were directly affected by the AI-2 quorum-sensing substance pool. Cumulatively, this suggested that biofilm formation in *S. sanguinis* is not under control of AI-2. Our study suggests that previously evaluated LuxS mutants in other species need to be revisited to resolve the precise contribution of AI-2 substance pools and the methionine pathways.

In 1979 it was demonstrated for the first time that a quorum sensing system worked across marine bacterial species (1). The mediator of this system, now known and commonly referred to as autoinducer-2 substance pool (AI-2),² was identified in several nonmarine, pathogenic bacteria (2, 3). Subsequently, the gene responsible for the generation of AI-2, *luxS*, was found to be widely conserved throughout the bacterial kingdom (4) and identified in a multitude of Gram-positive and Gram-negative, pathogenic and apathogenic bacteria (5, 6). Thus, the idea of an AI-2/LuxS-mediated interspecies communication was intensively discussed and suggested to play an essential role in development of virulence, especially biofilm formation (7–11).

LuxS together with Pfs represents an integral part of the activated methyl cycle (AMC) (Fig. 1), which provides activated methyl groups for the methylation of DNA, RNA, proteins and other substrates (5, 9, 12, 13). The LuxS/Pfs pathway, which is present in Gamma-, Beta-, and Epsilonproteobacteria as well as in Firmicutes (5), is responsible for the recycling of the toxic intermediate S-adenosylhomocysteine (SAH) to homocysteine.

Within this two-step enzymatic reaction, a byproduct occurs: the AI-2 substance pool precursor 4,5-dihydroxy-2,3-pentanedione (DPD) (14). Thus, the deletion of *luxS* to study the role of AI-2, would have two consequences: (i) the depletion of DPD, which is the desired phenotype, and (ii) a defect within the AMC caused by the interrupted LuxS/Pfs pathway, which could have additional effects on the phenotype and lead to misinterpretations of the role of AI-2. To circumvent this pitfall, it is necessary to study the effect of DPD depletion without affecting the AMC. One approach to accomplish this strategy is to bypass the interrupted LuxS/Pfs pathway by the SAH hydrolase (SahH), an alternative single-step reaction that catalyzes the conversion of SAH directly to homocysteine without the formation of DPD (5, 9, 12). This pathway exists within the AMC of Gamma-, Beta-, and Alphaproteobacteria, Chlorobia, Cya-

^{*}This work was supported by PathoGenoMic Plus Program Grant FKZ 0313801M and ERANet PathoGenoMics I Program Grant FKZ 0313936B from the German Federal Ministry of Education and Research.

^[5]This article contains supplemental Tables S1 and S2.

¹To whom correspondence should be addressed: Inst. of Medical Microbiology, Virology and Hygiene, University Hospital Rostock, Schillingallee 70, D-18057 Rostock, Germany. Tel.: 49-381-494-5950; Fax: 49-381-494-5902; E-mail: bernd.kreikemeyer@med.uni-rostock.de.

This is an Open Access article under the CC BY license.

²The abbreviations used are: AI-2, autoinducer-2; AMC, activated methionine cycle; BHI, brain heart infusion; CDM, chemical defined medium; DPD, 4,5-dihydroxy-2,3-pentanedione; SAH, S-adenosylhomocysteine; SahH, S-adenosylhomocysteine hydrolase; SAM, S-adenosyl-L-methionine; SRH, S-ribosylhomocysteine; THY, Todd-Hewitt broth supplemented with 0.5% yeast extract.

Heterologous *SahH* Restored AMC in *S. sanguinis luxS* Mutant

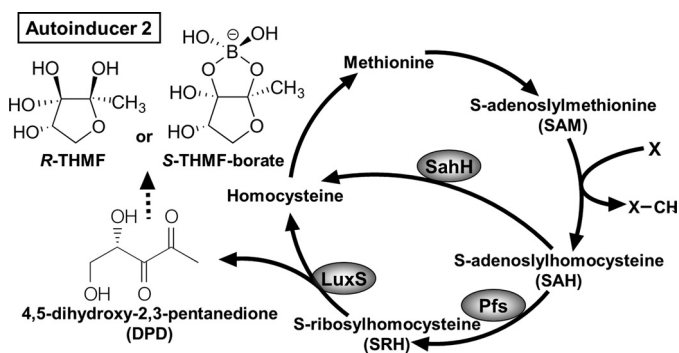


FIGURE 1. Schematic diagram of the AMC and the generation of the byproduct AI-2. Within the AMC the methyl donor SAM is generated from methionine by SAM synthetase (MetK, EC 2.5.1.6, SSA_1495) and recycled to methionine. SAM is needed to provide activated methyl groups for the methylation of DNA, RNA, proteins, and other substrates (X) by SAM-dependent methyltransferases (SSA_1812). The resulting toxic metabolite SAH is then converted in a single step directly to homocysteine via *SahH* (EC 3.3.1.1) or in a two-step conversion to *S*-ribosylhomocysteine (SRH) by a SAH nucleotidase (Pfs, EC 3.2.2.9, SSA_1639) and then to homocysteine by a *S*-ribosylhomocysteine lyase (LuxS, EC 4.4.1.21, SSA_1853), depending on the organism. Subsequently, homocysteine is recycled to methionine by the methionine synthase MetH (EC 2.1.1.13) or MetE (EC 2.1.1.14, SSA_0416) (5, 9, 12). A byproduct of the reaction catalyzed by LuxS is DPD, the precursor of AI-2. After spontaneous cyclization and hydration of DPD (2*R*,4*S*)-2-methyl-2,3,4-tetrahydroxytetrahydrofuran (*R*-THMF) is formed, a substance that shows AI-2 activity. Alternative cyclization, hydration, and subsequent reaction with boric acid leads to 3*A*-methyl-5,6-dihydro-furo(2,3-*d*)(1,3,2)dioxaborole-2,2,6,6-tetraol (*S*-THMF-borate), the first substance described as active AI-2 molecule (14, 66, 67). All genes indicated with a gene-ID ("SSA_XXXX") were found in *S. sanguinis* SK36. EC numbers and gene-IDs were assigned using Kyoto Encyclopedia of Genes and Genomes.

nobacteria, Bacteroidetes, and Actinobacteria, as well as in Archaea and Eukarya (5).

In the present study we investigated the complementation of the AMC in a *luxS* deletion mutant by heterologous expression of *Pseudomonas aeruginosa* *SahH*. The functionality of a *SahH* complemented interrupted AMC has been demonstrated only in Gram-negative bacteria (15, 16). Consequently, in our study we examined for the suitability of such heterologous complementation in a Gram-positive bacterium. This could be of broad interest because in several single and multispecies studies, especially on human pathogenic streptococci, a multitude of effects was observed, investigating *luxS* deletion mutants; in the exclusively human pathogen *Streptococcus pyogenes*, LuxS mutation had a pronounced effect on many virulence traits, including hemolytic and proteolytic activity as well as acid tolerance (17–19). Similar pleiotropic effects were observed in another important human pathogen, *Streptococcus pneumoniae*. A LuxS mutant was reduced in virulence with a defect in the ability to spread from initial colonization sites and to persist in nasopharyngeal tissue (20, 21). A down-regulation of natural competence and a severe defect in biofilm formation was also noted (22, 23).

The group of oral streptococci was intensively studied, because they mostly occur in biofilm structures in the oral cavity and have intensive contact to neighboring species, and thus, for them an interspecies communication via AI-2 could be crucial for survival. For example, it was postulated for *Streptococcus mutans*, the main cariogenic streptococcal species, that LuxS-dependent quorum sensing is involved in biofilm formation and acidic tolerance. Mutant-derived biofilms adopted a

more granular appearance (24), and *luxS*-deficient bacteria displayed an increased sensitivity to acidic killing (25). Culture filtrates of *Streptococcus gordoniae*, *Streptococcus sorbrinus*, and *Streptococcus anginosus* complemented the LuxS defect in *S. mutans*, whereas *Streptococcus oralis*, *Streptococcus salivarius*, and *Streptococcus sanguinis* filtrates had no effect (26). A reduced biofilm formation of strains with a defect in LuxS was further shown for *S. anginosus* (27), *S. gordoniae* (28, 29), and *Streptococcus intermedius* (30). In addition, a reduced mutualistic biofilm growth could be demonstrated for *S. oralis luxS* mutant in combination with *Actinomyces naeslundii* (8).

Complementation approaches in the mentioned species would be subject to the above described pitfall: Genetic complementation with homo- or heterologous *luxS* genes always restored all phenotypes; thus it was not possible to attribute all phenotypes to AI-2-based quorum sensing. The addition of external AI-2 did not always complement all observed effects, suggesting a central metabolic role of an intact AMC. This central role of LuxS in cellular metabolism was demonstrated for *S. mutans* by microarray analysis: up to 30% of the transcriptome was affected by the deletion of *luxS*; addition of AI-2 did not restore this effect (31, 32). These findings underscore the need of a tool for answering the question, if all the observed effects of LuxS deficiency were a result of the missing quorum sensing signal substance pool (AI-2) or a consequence of a defect in methionine metabolism (AMC).

In this study we focused on an inhabitant of the oral cavity. As a model we choose *S. sanguinis*, a member of the *S. sanguinis* group, and one of the causative agents of endocarditis (33–35).

We found a growth phase-dependent release of AI-2, which disappeared after deletion of *luxS*. The mutant was characterized by a changed *in vitro* biofilm phenotype compared with its WT strain. Therefore, in depth analyses of effects mediated by AI-2 and the lost LuxS activity were done, employing homologous *luxS* and heterologous *sahH* complementation analyses, chemical complementation, and DNA whole genome array based transcriptome experiments.

EXPERIMENTAL PROCEDURES

Bacterial Strains and Culture Conditions—Bacterial strains used in this study are listed in Table 1. *S. sanguinis* was grown on brain heart infusion (BHI; Oxoid, Wesel, Germany) agar or in BHI broth, aerobically supplemented with 5% CO₂ at 37 °C. Recombinant strains were cultured on BHI agar supplemented with erythromycin (5 µg ml^{−1}) or kanamycin (300 µg ml^{−1}), respectively. *Vibrio harveyi* was cultivated on LB (36, 37) agar or in autoinducer bioassay medium (1) at 30 °C aerobically. *Escherichia coli* was grown on LB agar or in LB at 37 °C aerobically. Recombinant *E. coli* strains were selected on LB agar supplemented with ampicillin (100 µg ml^{−1}), erythromycin (200 µg ml^{−1}), or kanamycin (30 µg ml^{−1}), respectively.

Setup for Biofilm Cultures—Preparatory cultures of all streptococcal strains were grown in BHI aerobically with 5% CO₂ at 37 °C to stationary phase. Bacteria were washed with PBS (pH 7.4) and adjusted to an A₆₀₀ of 0.6 to obtain 1 × 10⁸ cells/ml. Subsequently, each bacterial suspension was diluted 1:10 in a chemical defined medium (CDM) (38) supplemented with 50 mM sucrose (39) and inoculated in 96-Transwell polystyrene

TABLE 1

Bacterial strains and plasmids used in this study

The primers used for the generation of plasmids described in this study are given in supplemental Table S1.

Strains and plasmids	Relevant characteristics or distributions	Source or reference
Strains		
<i>Escherichia coli</i> DH5 α	Cloning host	Invitrogen (68)
<i>Pseudomonas aeruginosa</i> V14447	Wild type	Strain collection of the University Rostock (Germany)
<i>S. sanguinis</i> SK36	Wild type	American Type Culture Collection BAA-1455
<i>S. sanguinis</i> SR $\Delta luxS$	<i>luxS::ermAM</i>	This study
<i>S. sanguinis</i> SR $\Delta luxS/luxS$	<i>luxS::ermAM</i> ; pIB184Km- <i>luxS</i> -sang-TT _{BOB}	This study
<i>S. sanguinis</i> SR $\Delta luxS/sahH$	<i>luxS::ermAM</i> ; pIB184Km-P _{recA} - <i>sahH</i> -StrT-TT _{BOB}	This study
<i>Vibrio harveyi</i> MM77	<i>K_m^R</i> ; <i>luxLM::Tn5</i> ; <i>luxS::Cm^R</i> ; AI-1 [−] , Sensor AI-1 ⁺ ; AI-2 [−] , Sensor AI-2 ⁺	Ref. 42
Plasmids		
pASK IBA3	oriR (gram [−]); <i>Strep</i> -tag II [®] ; Amp ^R	IBA BioTAGnology GmBH
pAT19	oriR (gram ^{+/−}) (Stuttle Vector); Ery ^R	Ref. 69
pBluescript II KS ⁺	oriR (gram [−]); Amp ^R	Ref. 70
pIB184km	oriR (gram ^{+/−}) (Stuttle Vector); <i>K_m^R</i>	Ref. 71
pUC19	oriR (gram [−]); Amp ^R	Ref. 72
pUC19-Sang-Fu-ery	pUC19 containing <i>luxS</i> upstream (1200 bp), <i>luxS</i> downstream regions (1175 bp) of <i>S. sanguinis</i> SK36 and <i>ermAM</i> of pAT19	This study
pASK IBA3- <i>sahH</i>	pASK IBA3 containing <i>sahH</i> from <i>P. aeruginosa</i> V14447	This study
pIB184km-P _{recA} - <i>sahH</i> -StrT-TT _{BOB}	pIB184km containing an artificial transcription terminator, the promoter region of <i>recA</i> of <i>S. pyogenes</i> M2T2/44/RB4/119, <i>sahH</i> from pASK IBA3- <i>sahH</i> including <i>Strep</i> -tag II [®]	This study
pIB184km- <i>luxS</i> -sang-TT _{BOB}	pIB184km-TT _{BOB} containing <i>luxS</i> from <i>S. sanguinis</i> SK36	This study

microtiter plates (Corning Incorporated, Corning, NY). For safranin measurements uncoated 96-well plates (Greiner Bio-One, Frickenhausen, Germany) were used. To monitor pH, A_{600} , biofilm growth, cell viability, and AI-2 release over time, uncoated polystyrene 24-well plates (Greiner Bio-One) were used. Bacterial cultures were grown under static anaerobic conditions (80% N₂, 10% CO₂, 10% H₂) at 37 °C.

DNA Manipulations—Chromosomal DNA was isolated using the DNeasy Blood & Tissue Kit (Qiagen), PCR was performed using the Phusion high fidelity PCR system (Finnzymes, New England Biolabs), and endonuclease restriction was done with enzymes from Roche Applied Science according to manufacturer's instructions. Ligation with the Fast LinkTM DNA ligation kit (EPICENTRE[®] Biotechnologies, Madison, WI) was followed by transformation of competent *E. coli* (40). All recombinant plasmids were checked by sequencing (GATC Biotech, Konstanz, Germany).

Transformation *S. sanguinis*—*S. sanguinis* strains were grown to stationary phase in THY broth (Todd-Hewitt broth; supplemented with 0.5% yeast extract; Oxoid) aerobically supplemented with 5% CO₂ at 37 °C. Subsequently, bacterial cultures were diluted 1:20 in THY supplemented with glycine (20 mM) and grown to an A_{600} = 0.2–0.3. Cultures were chilled on ice for 10 min, washed twice in ice-cold electroporation buffer (0.3 M glucose), and suspended in 500 μ l of electroporation buffer. For electroporation, 150 μ l of competent cells were incubated on ice for 20 min in a 2-mm electroporation chamber (PEQLAB Biotechnology, Germany) with 5 μ g of plasmid. After electroporation (U = 1.75 kV; c = 25 μ F; r = 329 Ω ; t = 8.2 s), the cells were cooled on ice for 3 min, subsequently diluted in 1 ml of THY, and incubated at 37 °C for 1 h. The cells were plated on THY agar supplemented with erythromycin (5 μ g ml^{−1}) or kanamycin (300 μ g ml^{−1}) and incubated at 37 °C anaerobically for 48 h.

Deletion of *luxS*—The sequence of the *luxS* region *S. sanguinis* SK36 (accession number NC_009009.1) was used to design primers for amplification of *luxS* flanking regions (~1000 bp in length). PCR was done with the Phusion high fidelity PCR system. The primers Sang_up_for and Sang_up_rev were used for amplification of the *luxS* upstream fragment. For the downstream fragment primers Sang_down_for_2 and Sang_down_rev were applied, respectively (supplemental Table S1).

The downstream fragment was digested with XbaI/SphI and ligated into suicide vector pUC19. The resulting plasmid was named pUC19_Sang_down. Subsequently, the upstream fragment was digested with BamHI/SpeI and ligated into the digested pUC19_sang_down. The resulting plasmid was designated pUC19_Sang_Fu. Finally, the *ermAM* cassette was amplified using pAT19 as template and the primers ErmAM_for_Spe and ErmAM_rev_Spe. The amplified DNA was digested with SpeI and ligated into digested pUC19_Sang_Fu. The resulting plasmid pUC19-Sang-Fu-ery was used for transformation of *S. sanguinis* SK36, thereby obtaining *S. sanguinis* SR $\Delta luxS$. Double crossover events were selected on THY agar supplemented with 5 μ g ml^{−1} erythromycin. Transformants were checked for correct substitution of *luxS* with *ermAM* by PCR and Southern blotting (data not shown).

Complementation of *S. sanguinis* SR $\Delta luxS$ with Heterologous *sahH*—To control against polar effects, the artificial transcription terminator TT_{BOB} was introduced into pIB184km. In previous experiments, the functionality of TT_{BOB} was demonstrated (data not shown). The sequence was synthesized by Eurogentec GmbH (Cologne, Germany): GCATGCaatcaataaaataaaattggcagcgactactacaagtagcgtccgtgccatattgttattatttACATGC. Underlining indicate the attached restriction sites for SphI/NspI and the complementary sequences forming the hairpin loop. TT_{BOB} was digested with NspI, recognizing the sequence RCATGY and producing the SphI-compatible

sticky ends. TT_{BOB} was subcloned adjacent to the multiple cloning site of pAT19 via SphI to receive the following fragment: 5'-EcoRI-multiple cloning site-SphI-TT_{BOB}-HindIII-3'. This modified multiple cloning site was amplified by PCR using the primers M13_FP and M13_RP_XhoI. The product was subsequently digested with BamHI/XhoI and ligated into the digested pIB184km, obtaining pIB184km-TT_{BOB}.

P_{recA}, a constitutively active promoter of *S. pyogenes* routinely used in our laboratory, was cloned into pIB184km-TT_{BOB} using the primers Prec_for_Ma_Sac and Prec_rev_Sy_Bam, obtaining pIB184km-P_{recA}-TT_{BOB}.

sahH was amplified by PCR using the primers SahH_for_Pap_Not, SahH_rev_Pap_Not (15), and chromosomal DNA of *P. aeruginosa* V14447. The product was subcloned into pBluescriptII KS⁺ for sequencing, subsequently amplified with Sah_over_Eco_for and Sah_over_Pst_rev, EcoRI/PstI-digested, and ligated into pASK-IBA3. Finally, *sahH* was amplified from pASK-IBA3-*sahH* by PCR using Sah_pAT_F_Bam and Sah_StT_TT_Sph. The resulting DNA fragment was BamHI/SphI-digested and cloned into pIB184km-P_{recA}-TT_{BOB}. Detailed sequence information of all primers is contained in supplemental Table S1.

S. sanguinis SR Δ luxS was finally transformed with pIB184km-P_{recA}-*sahH*-StrT-TT_{BOB} obtaining *S. sanguinis* SR Δ luxS/*sahH*. The presence of the active enzyme was demonstrated according to the quality control test procedure outlined in the product information sheet provided by Sigma (enzymatic assay for SahH, EC 3.3.1.1; data not shown).

Complementation of *S. sanguinis* SR Δ luxS—*luxS*, including its natural promoter, was amplified by PCR using chromosomal DNA of *S. sanguinis* SK36 and employing primers Kom_Lux_sang_F plus Kom_Lux_Sang_R (supplemental Table S1). The plasmid pIB184km-TT_{BOB} was ApaI/SphI-digested and ligated with the digested *luxS* fragment. *S. sanguinis* SR Δ luxS was then transformed with pIB184km-*luxS*-sang-TT_{BOB} obtaining *S. sanguinis* SR Δ luxS/*luxS*.

Safranin Assay—Bacterial cells were grown in uncoated polystyrene 96-well microtiter plates (Greiner Bio-One, Frickenhausen, Germany). After incubation for 24 h under anaerobic conditions at 37 °C, liquid medium was removed, and the wells were washed gently with PBS to remove nonadherent sedimented cells. For determination of biofilm mass, the wells were stained with 0.1% safranin for 15 min, washed with PBS, and air-dried. Biofilm mass was quantified by measuring the absorbance at 492 nm against 620-nm reference with a microplate reader (Tecan reader).

For Transwell studies, uncoated 96-Transwell polystyrene microtiter plates (Corning) were used, containing 200 μ l of the first and 50 μ l of the second bacterial strain in the lower and upper compartments, respectively. After incubation for 24 h at 37 °C under anaerobic conditions, Transwell inserts and medium were removed, and biofilms were analyzed by safranin stain as mentioned above.

Crystal Violet Assay—For determination of biofilm growth over time, bacterial cells were grown in uncoated 24-well plates (Greiner Bio-One). Liquid medium was removed at hourly intervals, and wells were washed gently with PBS. Biofilm cells were stained with 0.5 ml of 0.1% crystal violet for 15 min,

washed with PBS, and air-dried. Crystal violet stain was removed with 1 ml of 1% SDS for 15 min of agitation. Before determination of A₅₄₀, the solution was diluted 1:10 with 1% SDS.

Autoinducer-2 Bioassay—*S. sanguinis* strains were cultured in uncoated polystyrene 24-well plates (Greiner Bio-One) as mentioned above. One-ml culture was removed every hour and centrifuged, and the sterile filtered (0.2- μ m pore size; Sterifix, Braun) cell-free supernatant was stored at -20 °C until measurement. The detection of AI-2 was performed as previously described (6, 41) with slight modification. *V. harveyi* MM77 (42) was used as the reporter strain because this strain does not produce AI-1 nor AI-2. Thus, it should show no autoluminescence, which was confirmed by our test system (data not shown). Luminescence was measured using a Spectramax M2 (Molecular Devices). For quantification of AI-2 concentration in culture samples, artificial AI-2 (DPD; Omm Scientific) was added on every tested 96-well plate in a graded dilution of 0.025–50 μ M, serving as positive control and to plot a standard curve.

Scanning Electron Microscopy—For a qualitative documentation of biofilm architecture, bacterial cells were cultured in uncoated polystyrene 24-well plates (Greiner Bio-One) as mentioned above. Each well contained an uncoated, sterile plastic coverslip (13-mm diameter; Nunc, Wiesbaden, Germany). After 24 h, biofilms on coverslips were fixed for 24 h in 2.5% glutaraldehyde, subsequently washed with 0.1 M sodium acetate buffer (pH 7.3) and dehydrated in a graded series of ethanol. Coverslips were subjected to critical point drying with CO₂, sputter-coated with gold (thickness, ~10 nm), and examined with a Zeiss DSM 960A electron microscope.

Transcriptome Analysis—*S. sanguinis* was grown in CDM/sucrose under anaerobic conditions in uncoated CELLSTAR® tissue culture flasks (75 cm², 250 ml; Greiner Bio-One, Frickenhausen, Germany). For analysis of gene regulation depending on AI-2, DPD was added after 5.5 and 7 h of growth to gain a final concentration of 4.5 and 9 μ M, respectively. Cells were harvested and washed with PBS after 8 h of growth, meaning at the end of transient growth phase and after the AI-2 release in *S. sanguinis* WT reached its maximum.

RNA preparation was carried out from 100 mg of cell material (wet weight) with the Fast RNA® Pro Blue kit (MP Biomedicals, Solon, OH) following the manufacturer's instructions. cDNA synthesis, labeling, hybridization, scanning, feature extraction, and quality control of the arrays were essentially done as previously described (43). Normalization and background correction was done with NimbleScan Software using the RMA (robust multiarray analysis (44)).

The resulting data (log2) were statistically analyzed with GeneSpring GX (version 11.0; Agilent Technologies, Waldbronn, Germany). One-way ANOVA (45) was used for the significance analysis of *S. sanguinis* SR Δ luxS compared with *S. sanguinis* SK36 and *S. sanguinis* SR Δ luxS/*sahH*. A *t* test was performed for analysis of *S. sanguinis* SR Δ luxS/*sahH* with and without the addition of DPD. In all cases a *p* value of *p* ≤ 0.05 was used (multiple testing correction: Benjamini-Hochberg (46)).

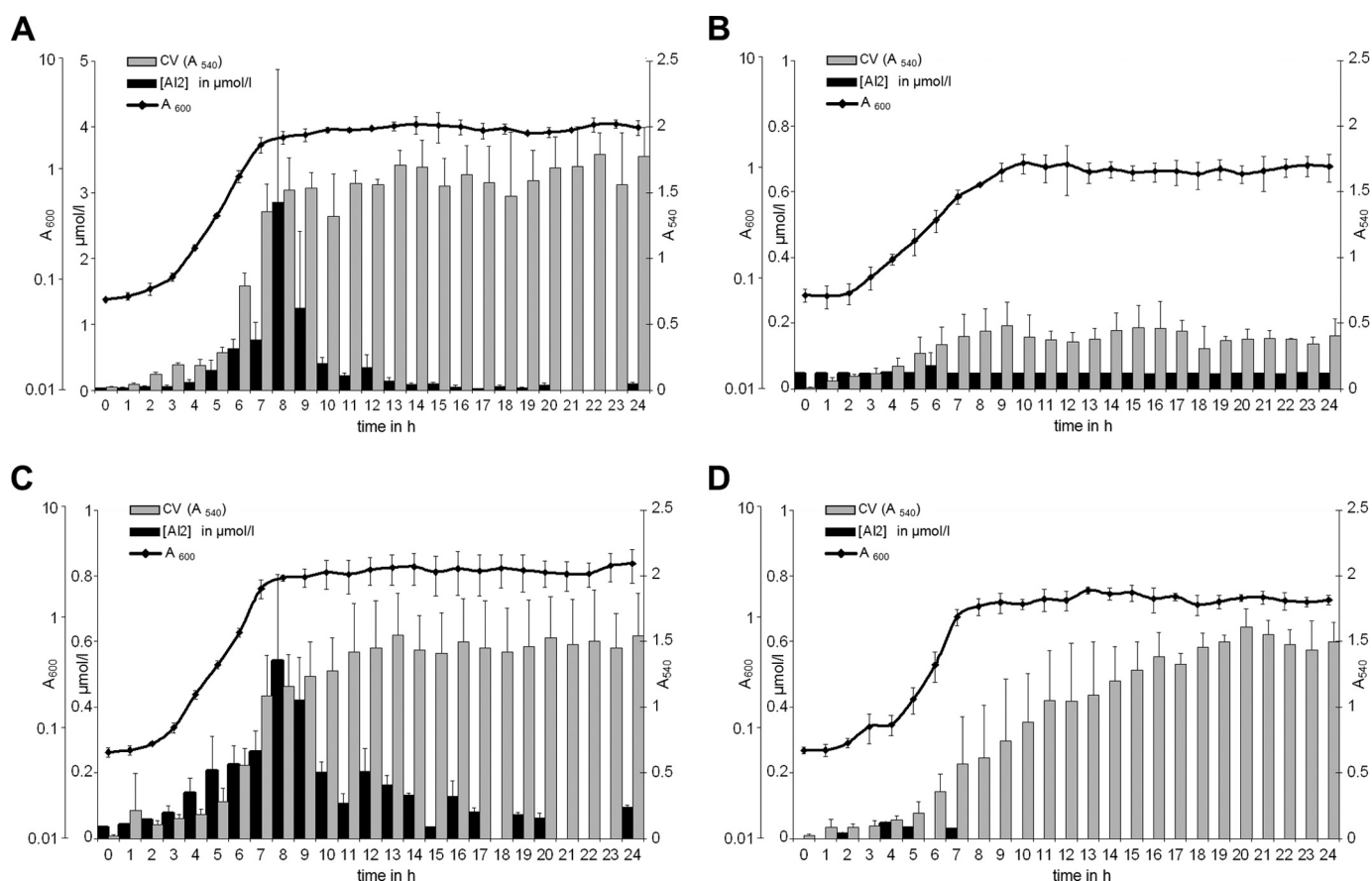


FIGURE 2. AI-2 concentration, biofilm mass, and optical density of investigated *S. sanguinis*. A–D, *S. sanguinis* SK36 (A), its *luxS* deletion mutant *S. sanguinis* SR $\Delta luxS$ (B), the *luxS* complemented strain *S. sanguinis* SR $\Delta luxS/luxS$ (C), and the transgenic complemented strain *S. sanguinis* SR $\Delta luxS/sahH$ (D). Bacterial cells were grown anaerobically in CDM/sucrose. Optical density (line with points A_{600} ; left y axis), AI2 concentration (black bars [AI2]; second y axis), and biofilm mass (gray bars A_{540} ; crystal violet stain; right y axis) were determined hourly. The error bars indicate standard deviation. Please note the different graduation of the secondary y axis in Fig. 2A.

Competence Assay—A transformation assay was performed as previously described by Merritt *et al.* (47) with slight modifications. *S. sanguinis* strains were cultured overnight in competence medium (Todd-Hewitt broth; supplemented with 0.4% BSA) and subsequently 1:30 diluted in fresh competence media with and without the addition of DPD (4.5 μM). After the culture reached an A_{600} of ~ 0.2 , DPD addition was repeated (9 μM). Simultaneously, linearized plasmid DNA (20 $\mu g ml^{-1}$) was added to each culture, conferring a tetracycline resistance. Prior to the transformation, the transforming plasmid pFW2 (48) was BamHI-digested. Subsequently, the cultures were allowed to grow for an additional 2 h and were then plated on BHI agar supplemented with tetracycline (5 $\mu g ml^{-1}$) as well as on nonselective BHI plates. Transformation efficiency was defined as the ratio of transformants/total viable cells (47).

Reproducibility and Statistics—Each experiment was performed on at least three independent occasions (biological replicates) with two or three replicates each (technical replicates). The statistical parameters (mean, standard deviation, and *p* values) and tests were determined employing the following software: GenSpringGX 11.0, SoftMax Pro 5.4, and Windows Excel. *p* values less than 0.05 were considered as significant.

Accession Numbers—The raw data and meta information of the DNA array-based transcriptome experiments have been deposited in GEO database (accession number GSE37007). The

nucleotide sequence information of *sahH* from *P. aeruginosa* V14447 have been placed on NCBI database with the accession numbers JQ894861.

RESULTS

The AI-2 Release Is Growth Phase-dependent—*S. sanguinis* was cultured anaerobically in CDM/sucrose. These growth conditions proved to be optimal for biofilm formation (39). We quantified AI-2 under the selected conditions, monitored its release for 24 h, examined the A_{600} , and determined the biofilm mass. The maximum amount of AI-2 ($\sim 2.9 \mu M$) was found in the early stationary growth phase in the *S. sanguinis* culture after the biofilm mass reached its maximum (Fig. 2A).

The Deletion of *luxS* Significantly Affects Biofilm Formation in *S. sanguinis*—Based on the published full genome sequence of *S. sanguinis* SK36, we generated the *luxS* deletion mutant *S. sanguinis* SR $\Delta luxS$. The phenotype of the *luxS* mutant was investigated under anaerobic conditions in CDM/sucrose. Biofilm masses were analyzed by safranin staining after 24 h of growth. The *S. sanguinis* SR $\Delta luxS$ mutant displayed significantly altered biofilm structures compared with its parental WT strain (*p* < 0.001) (Fig. 3, left pair of columns). Identical results were obtained either using safranin or crystal violet staining procedures (Fig. 2B). To rule out a reduced biofilm mass simply as a consequence of diminished growth caused by

Heterologous *SahH* Restored AMC in *S. sanguinis luxS* Mutant

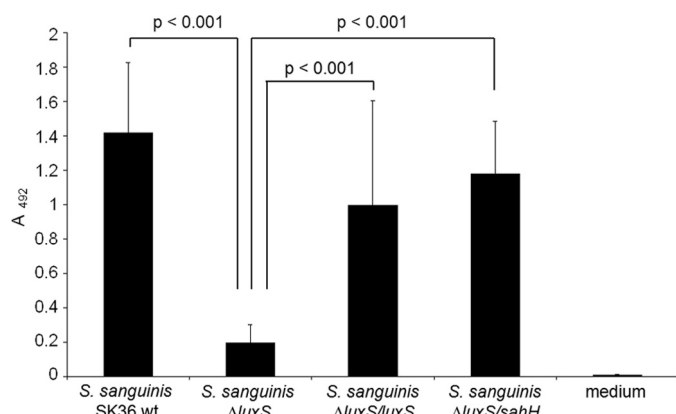


FIGURE 3. Biofilm mass of *S. sanguinis*. SK36, *S. sanguinis* SR $\Delta luxS$, *S. sanguinis* SR $\Delta luxS/luxS$, and *S. sanguinis* SR $\Delta luxS/sahH$ were grown for 24 h anaerobically in CDM/sucrose. Depicted is the absorbance at 492 nm of safranin-stained biofilms. The error bars indicate standard deviation. Differences in biofilm mass of *S. sanguinis* SR $\Delta luxS$ was highly significant compared with its parental WT strain *S. sanguinis* SK36 ($p = 9.31E-8$; $n = 11$), after complementation of *luxS* (*S. sanguinis* SR $\Delta luxS/luxS$; $p = 2.79E-6$; $n = 11$), and after transgenic complementation with *sahH* (*S. sanguinis* SR $\Delta luxS/sahH$; $p = 9.31E-8$; $n = 11$). Significance was determined by two-tailed *U* test.

the *luxS* deletion, the A_{600} and viability of the mutant and wild type strains were monitored for 24 h. The growth curves (Fig. 2, A and B) and viable cell counts (data not shown) of both strains were similar. These results corresponded well with the staining experiments, because safranin predominantly interacts with the intercellular matrix, and crystal violet is directed to the cellular components of a biofilm. Thus, the deletion of *luxS* caused a reduction of biofilm mass of *S. sanguinis* SR $\Delta luxS$ but did not affect the bacterial growth rates or viable cell count. The AI-2 concentrations in all cultures of the *luxS* deletion mutant were reduced, demonstrating that functional deletion of *luxS* in final consequence leads to deletion of DPD production and thus AI-2 substance pool depletion.

Plasmid Encoded *luxS* Restored WT Phenotype of *S. sanguinis* SR $\Delta luxS$ —With the *S. sanguinis* SR $\Delta luxS$ strain at hand, we now had the tools to investigate the individual contributions of an AI-2 deficiency and methionine deficiency for the observed phenotype of the *S. sanguinis* SR $\Delta luxS$ mutant.

First, the *S. sanguinis* SR $\Delta luxS$ strain was complemented with a plasmid encoding *luxS* of its parental WT strain, with the intention to restore both, the AI-2 substance pool formation and the complete methionine pathway (Fig. 1). The complemented strain *S. sanguinis* SR $\Delta luxS/luxS$ was investigated by AI-2 measurement, scanning electron microscopy, crystal violet, and safranin stain. The AI-2 release as well as the biofilm architecture was restored to WT level (Figs. 2C, 3, and 4), demonstrating that the observed effects in *S. sanguinis* SR $\Delta luxS$ were caused by a single gene deletion.

Biofilm Mass Production of *S. sanguinis* Is Independent from AI-2 Substance Pools—Several previous studies postulated AI-2 substances as key players in single and mixed species biofilm development (7, 8, 49). Thus, in the next set of experiments we studied the individual role of the AI-2 compound on *S. sanguinis* biofilm formation. The ability of AI-2 to restore the *S. sanguinis* SR $\Delta luxS$ biofilm back to WT level was investigated by two approaches. First, artificial AI-2 (DPD) was added directly to the growth medium of the *S. sanguinis* SR $\Delta luxS$ strain. Con-

centrations of DPD were selected to match the physiological range, which was defined by quantification of AI-2 release over the time in the previous experiments of this study (Fig. 2A). The resulting biofilm mass of *S. sanguinis* SR $\Delta luxS$ was not influenced by the addition of 1, 5, and 25 μM DPD (Fig. 5A), although former studies and control experiments in our laboratory proved that active AI-2 substances can be formed from this precursor (31, 50) (standard curve with the artificial DPD (data not shown)).

Second, *S. sanguinis* SR $\Delta luxS$ was co-cultured with its parental WT strain in a Transwell test system, which enables the exchange of small molecules but prevents direct cell contact. Also, with this assay setup we found no significant differences in biofilm mass. AI-2 produced by the WT strain in the upper compartment did not elevate the biofilm mass of *S. sanguinis* SR $\Delta luxS$ in the lower compartment (Fig. 5B).

These two strategies revealed that neither external addition of AI-2 (DPD), nor WT supernatant were able to complement the attenuated biofilm architecture of *S. sanguinis* SR $\Delta luxS$, thereby indicating that biofilm formation in *S. sanguinis* is independent of AI-2 substance pools. Consequently, the hampered biofilm forming capacity of the *S. sanguinis* SR $\Delta luxS$ mutant could be a result of a defect in methionine metabolism caused by the missing LuxS activity (Fig. 1).

Transgenic *sahH* Restored WT Biofilm Phenotype of *S. sanguinis* SR $\Delta luxS$ —Next we introduced transgenic *sahH* into *S. sanguinis* SR $\Delta luxS$ to bypass the Pfs/LuxS pathway within the AMC. The resulting transgenic *sahH* strain *S. sanguinis* SR $\Delta luxS/sahH$ was tested for its AI-2 release. Moreover, the A_{600} , cell viability, and biofilm mass were monitored for 24 h. The growth and the biofilm development were similar to the wild type strain culture, although no AI-2 release was detectable (Fig. 2D). After a 24-h culture period, the biofilm mass of the *sahH*-complemented strain was significantly different compared with *S. sanguinis* SR $\Delta luxS$ ($p < 0.001$). It formed biofilm masses similar to those of the parental WT and the *luxS* complemented SR $\Delta luxS/luxS$ strain (Fig. 3). Thus, transgenic *sahH* alone restored WT biofilm in a *luxS* mutant of *S. sanguinis*. This strongly suggests that a defect in methionine production in a *luxS* mutant background is the primary factor responsible for the attenuated biofilm phenotype. However, indirect and not readily predictable factors and mechanisms could also play a role.

Electron Microscopy of *S. sanguinis* SR $\Delta luxS/sahH$ —To verify the restoration of WT biofilm phenotype and to rule out a changed cell shape, *S. sanguinis* strains were investigated by scanning electron microscopy (Fig. 4). Moreover, this technique allowed a qualitative evaluation of biofilm architecture. The cells were grown for 24 h on uncoated, sterile plastic coverslips in CDM/sucrose and examined with a Zeiss DSM 960A electron microscope.

S. sanguinis SR $\Delta luxS/sahH$ (Fig. 4, J–L) and *S. sanguinis* SR $\Delta luxS/luxS$ (Fig. 4, G–I) formed solid biofilms, similar to the WT culture (Fig. 4, A–C). All three strains were able to cover the surface of carrier material completely, resulting in dense biofilms. Compared with the biofilms of the parental WT strain, the *luxS*, or the *sahH* complemented *luxS* mutants (Fig. 4, D–F), biofilms of *S. sanguinis* SR $\Delta luxS$ were reduced in com-

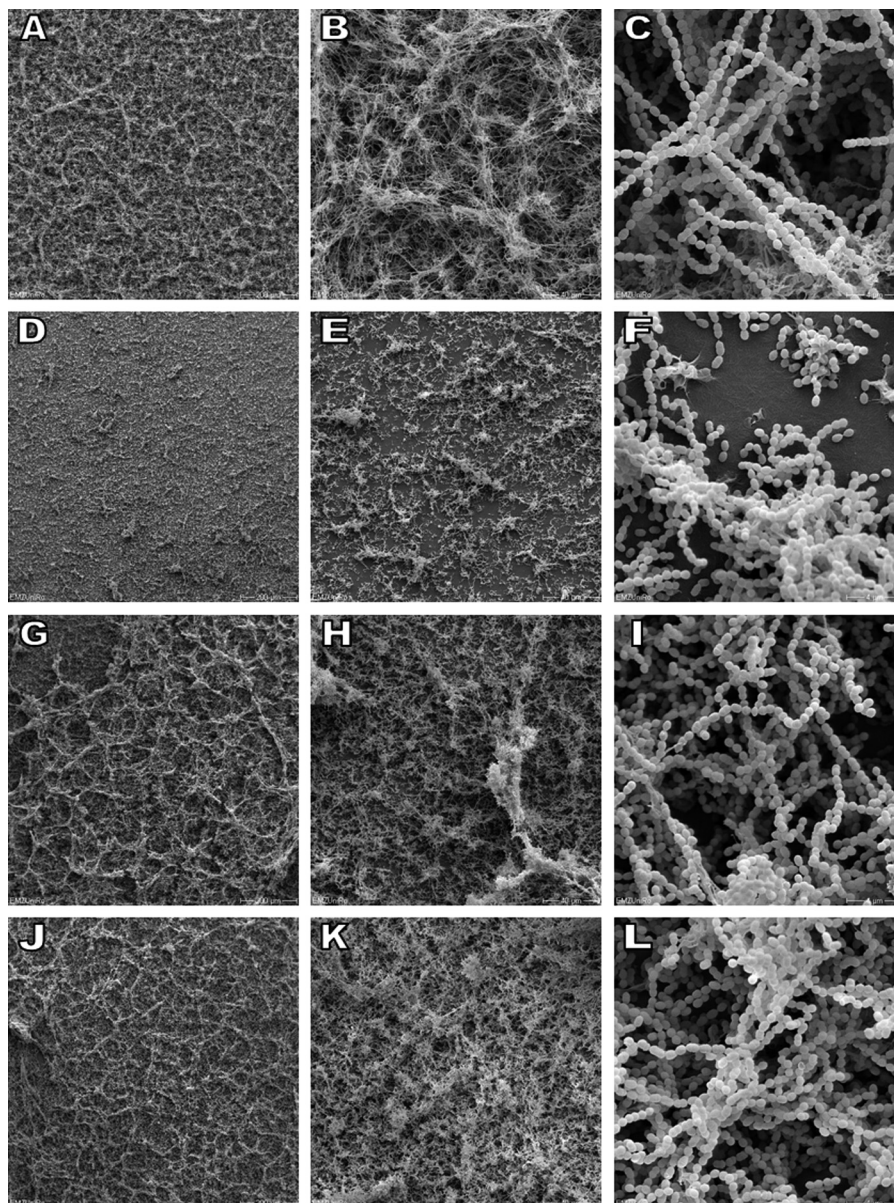


FIGURE 4. Scanning electron microscopy images of *S. sanguinis* biofilms: *S. sanguinis* SK36 (A–C), *S. sanguinis* SR $\Delta luxS$ (D–F), *S. sanguinis* SR $\Delta luxS/luxS$ (G–I), and *S. sanguinis* SR $\Delta luxS/sahH$ (J–L). Cells were grown for 24 h anaerobically in CDM/sucrose on uncoated, sterile plastic coverslips. Coverslips with biofilms were examined with a Zeiss DSM 960A electron microscope with the following magnifications: 100 \times (A, D, G, and J), 500 \times (B, E, H, and K), and 5000 \times (C, F, I, and L).

plexity and compactness. No differences in cell morphology or cell arrangement were detectable.

Genome Wide Transcriptome Analysis Confirmed Metabolic Complementation by Transgenic *SahH*—The previous experiments of this study demonstrated a recovery of natural biofilm masses and architecture in the *S. sanguinis* SR $\Delta luxS$ strain by transgenic complementation with *sahH* but not by addition of AI-2.

In the next set of experiments, we investigated the genome wide influence of the *luxS* deletion and the transgenic *sahH* complementation by comparative transcriptome analysis employing a recently developed and validated array platform (43). The aim was to investigate whether the heterologous expression of *sahH* also complemented transcriptional changes of the *luxS* deletion.

The cells were cultured anaerobically in CDM/sucrose and harvested after 8 h of growth. At this time point AI-2 release of *S. sanguinis* WT had reached its maximum; therefore, we expected a maximum difference in gene expression. The data sets from *S. sanguinis* SR $\Delta luxS/sahH$ and *S. sanguinis* SK36 were compared with *S. sanguinis* SR $\Delta luxS$.

Using a fold change cutoff level of ≥ 3 , 216 genes were identified to be differentially transcribed. Regarding their metabolic function, they were grouped into five classes and 19 subclasses. Several genes are mentioned in multiple categories; however, they were not counted in multiples for the calculation of the total number of differentially transcribed genes. Gene expression changes were displayed in a color-coded manner in Table 2 (precise values are shown in supplemental Table S2). Among the genes with differential transcript abundance, we identified

Heterologous *SahH* Restored AMC in *S. sanguinis luxS* Mutant

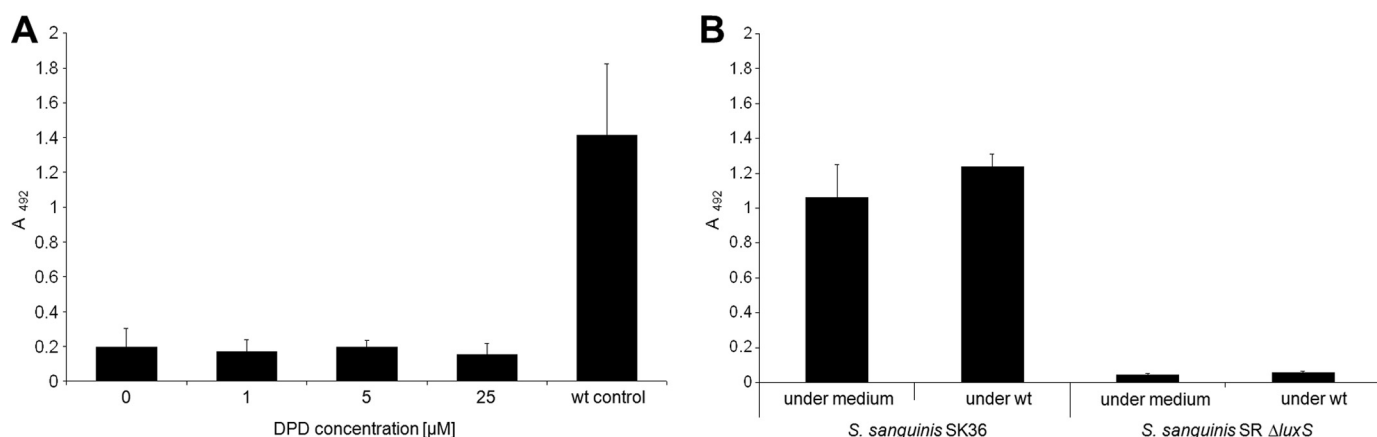


FIGURE 5. **Biofilm mass of *S. sanguinis*.** SK36 *luxS* mutant and its parental WT strain were grown for 24 h anaerobically in CDM/sucrose. Shown is the absorption of safranin-stained biofilms (492 nm). The error bars indicate standard deviations. **A**, *S. sanguinis* SR $\Delta luxS$ was cultivated with different concentrations of DPD (AI-2) in its culture medium. Furthermore, a WT control was cultured without the addition of DPD. **B**, *S. sanguinis* SK36 and *S. sanguinis* SR $\Delta luxS$ were cultivated in the lower compartment of a Transwell system under a WT culture or medium control in the upper compartment, respectively.

TABLE 2

Kyoto Encyclopedia of Genes and Genomes class prediction of regulated genes of WT and *sahH* complemented *luxS* mutant compared with *S. sanguinis* SR $\Delta luxS$

Total RNA of *S. sanguinis* cultures was isolated after 8 h of growth and used for transcriptome analysis. The data sets were analyzed with the one-way ANOVA software. Genes with a fold change of ≥ 3 in at least one of two conditions (WT versus *luxS* mutant; *sahH* complemented *luxS* mutant versus *luxS* mutant) were grouped regarding their metabolic function according to Kyoto Encyclopedia of Genes and Genomes. Depending on their function, several genes might appear in multiple functional categories. The resulting up- or down-regulation was color-coded as indicated below.

Seq_ID	Gene	WT vs $\Delta luxS$	$\Delta luxS/sahH$ vs $\Delta luxS$	Seq_ID	Gene	WT vs $\Delta luxS$	$\Delta luxS/sahH$ vs $\Delta luxS$	Seq_ID	Gene	WT vs $\Delta luxS$	$\Delta luxS/sahH$ vs $\Delta luxS$	Seq_ID	Gene	WT vs $\Delta luxS$	$\Delta luxS/sahH$ vs $\Delta luxS$		
Cellular Processes				Genetic Information Processing				Metabolism				Metabolism				Unclassified	
Signaling: Cell motility and Cell growth				Folding, Sorting, Degradation				Amino Acid Metabolism				Lipid Metabolism				Poorly Characterized	
SSA_1038				SSA_0015	<i>ftsH</i>			SSA_0068	<i>adhE</i>			SSA_0657					
SSA_1775	<i>trkA</i>			SSA_0312	<i>trdH</i>			SSA_0631	<i>trdH</i>			SSA_0684					
SSA_1547	<i>trkK</i>			SSA_0836	<i>secA2</i>			SSA_0737	<i>trpP</i>			SSA_0800	<i>cobO</i>				
SSA_0655	<i>ftsA</i>			SSA_0836	<i>emo</i>			SSA_0977	<i>leuB</i>			SSA_0817					
SSA_0656	<i>ftsZ</i>			SSA_1069	<i>lndA</i>			SSA_0980	<i>leuC</i>			SSA_1125					
SSA_1298	<i>malX</i>			SSA_2007	<i>dnaK</i>			SSA_0981	<i>leuD</i>			SSA_1307	<i>rrkH2</i>				
SSA_2302				SSA_2049	<i>mmpA</i>			SSA_1013				SSA_1513	<i>renF</i>				
SSA_0721	<i>sodA</i>			SSA_2096	<i>cinL</i>			SSA_1467	<i>aroC</i>			SSA_1514					
Environmental Information Processing				SSA_2005	<i>dnaJ</i>			SSA_1942	<i>rhaB</i>			SSA_1553					
Membrane Transport				SSA_2052				SSA_2048	<i>cvsE</i>			SSA_1558					
SSA_0221				SSA_2208	<i>secE</i>			SSA_2063	<i>penS</i>			SSA_1605	<i>nmrA</i>				
SSA_0376				SSA_0100	<i>rodA</i>			SSA_2173	<i>hnsO</i>			SSA_1762					
SSA_0477	<i>cbiM</i>			SSA_0355	<i>mutS</i>			SSA_0046	<i>nurB</i>			SSA_1780	<i>xerD</i>				
SSA_0772	<i>ntslH</i>			SSA_0549	<i>recG</i>			SSA_1555	<i>adh</i>			SSA_1804					
SSA_0834				SSA_0655	<i>ftsA</i>			SSA_1784	<i>murI</i>			SSA_1897					
SSA_0836	<i>secA2</i>			SSA_0656	<i>ftsZ</i>			SSA_1942	<i>rhaB</i>			SSA_2211					
SSA_0929				SSA_0660	<i>divF</i>			SSA_2332	<i>dlcC</i>			SSA_2221					
SSA_0942	<i>mtcC</i>			SSA_0824	<i>dhcG</i>			SSA_1865				SSA_2278	<i>canD</i>				
SSA_0943	<i>mtcC</i>			SSA_0875	<i>rodA</i>			SSA_0553				SSA_2333	<i>ubiA</i>				
SSA_1027				SSA_1220	<i>gvrA</i>			SSA_0068	<i>adhE</i>			SSA_0141	<i>dlbB</i>				
SSA_1040				SSA_1626	<i>trkK</i>			SSA_0778				SSA_0326					
SSA_1048	<i>notA</i>			SSA_1778	<i>scnB</i>			SSA_0788				SSA_0539					
SSA_1298	<i>malX</i>			SSA_1805	<i>dhcA</i>			SSA_0221				SSA_0418					
SSA_1299	<i>malF</i>			SSA_1859	<i>recL</i>			SSA_0271				SSA_0593					
SSA_1359				SSA_2066	<i>poC</i>			SSA_0302	<i>pok</i>			SSA_1309					
SSA_1507	<i>renD</i>			SSA_0214	<i>ssb2</i>			SSA_0886	<i>eno</i>			SSA_1745	<i>csdH</i>				
SSA_1508	<i>renC</i>			SSA_0448	<i>avrA</i>			SSA_0980	<i>leuB</i>			SSA_1957	<i>renC</i>				
SSA_1726	<i>livG</i>			SSA_0981	<i>mus</i>			SSA_1012				SSA_2191	<i>ntrK</i>				
SSA_1918				SSA_0176	<i>rodA</i>			SSA_1212	<i>trpS</i>			Unknown					
SSA_1919				SSA_0177	<i>rodA</i>			SSA_1521	<i>nuc</i>			SSA_0101					
SSA_1920				SSA_0678	<i>adhE</i>			SSA_1555	<i>adh</i>			SSA_0167					
SSA_1945				SSA_1000	<i>galP</i>			SSA_1918				SSA_0258					
SSA_1946				SSA_2200	<i>ctsR</i>			SSA_1919				SSA_0591					
SSA_2302				SSA_2009	<i>hcrA</i>			SSA_1920				SSA_0672					
SSA_1913				SSA_0115	<i>romC</i>			SSA_1932	<i>accC</i>			SSA_0745					
SSA_2166				SSA_0120	<i>romG</i>			SSA_1934	<i>accB</i>			SSA_0811					
SSA_2208	<i>secE</i>			SSA_0133	<i>romG</i>			SSA_1942	<i>rhaB</i>			SSA_0983					
SSA_0677	<i>hivA</i>			SSA_0744	<i>ancA</i>			SSA_1893				SSA_1429					
Signaling Molecules and Interaction				SSA_1223	<i>romC</i>			SSA_0086	<i>ntpK</i>			SSA_1559					
				SSA_1377	<i>ancS</i>			SSA_0784	<i>uncF</i>			SSA_1782					
				SSA_1430	<i>elaC</i>			SSA_0785	<i>uncH</i>			SSA_2047					
				SSA_2044	<i>chs</i>			SSA_0886	<i>eno</i>			SSA_2197					
				SSA_2109	<i>hcrA</i>			SSA_1012				SSA_2198					
				SSA_2110	<i>romG</i>			SSA_1503	<i>fer</i>			SSA_2279					
				SSA_0820	<i>rstU</i>			SSA_1521	<i>nuc</i>			SSA_2299					
				SSA_1032	<i>rstU</i>			SSA_1953	<i>nifU</i>			SSA_2300					
				SSA_1272	<i>rmrE</i>			SSA_2048	<i>cvsE</i>			SSA_2320					
								SSA_0140	<i>cinA</i>			SSA_2320					
								SSA_0088	<i>ntpC</i>			SSA_1354					
								SSA_0092	<i>ntpB</i>			SSA_2276					
								SSA_0093	<i>ntpD</i>			SSA_0360					
								Energy Metabolism				Others					
								SSA_0271				SSA_0015	<i>ftsH</i>				
								SSA_0689	<i>phbB</i>			SSA_0068	<i>adhE</i>				
								SSA_0861	<i>murN</i>			SSA_0077					
								SSA_0862	<i>murM</i>			SSA_1846	<i>ppnL</i>				
								SSA_1509	<i>renB</i>			SSA_1942	<i>rhaB</i>				
								Glycan Biosynthesis and Metabolism				Metabolism of Terpenoids and Polyketides					
								SSA_0271			SSA_0334	<i>malK2</i>					
								SSA_0689	<i>phbB</i>			SSA_0335	<i>malK2</i>				
								SSA_0861	<i>murN</i>			SSA_1906					
								SSA_0862	<i>murM</i>			SSA_1931	<i>accD</i>				
								SSA_1509	<i>renB</i>			SSA_1932	<i>accC</i>				
												SSA_1934	<i>accB</i>				
												SSA_1942	<i>rhaB</i>				
												SSA_0337					
												Poorly Characterized					
												SSA_0077	<i>glt</i>				
												SSA_0303	<i>ssuC</i>				
												SSA_0590					
												SSA_0587					
												SSA_0763	<i>nerO</i>				
												Unclassified					
												Poorly Characterized					
												SSA_0077	<i>glt</i>				
												SSA_0303	<i>ssuC</i>				
												SSA_0590					
												SSA_0587					
												SSA_0763	<i>nerO</i>				

fold change

up

regulated

down regulated

1 - 2

2 - 3

4 - 5

> 5

TABLE 3

S. sanguinis SR $\Delta luxS/sahH$ genes with altered transcript amounts upon AI-2 addition

Total RNA of *S. sanguinis* SR $\Delta luxS/sahH$ cultured with and without the addition of DPD was used for transcriptome analysis. The data sets were analyzed with a *t* test (multiple testing correction: Benjamini-Hochberg corrected *p* value of $p \leq 0.05$). Displayed are genes with a fold change of ≥ 3 .

GeneID	Gene name/description	Fold change
Up-regulated		
SSA_0019	pcsB/secreted antigen GbpB/SagA; peptidoglycan hydrolase; PcsB protein precursor, putative	3.47
SSA_0184	comYA/competence protein ComYA, putative	3.07
SSA_0185	comYB/competence protein ComYB, putative	3.7
SSA_0188	Conserved hypothetical protein	3.44
SSA_0189	Competence protein ComGF, putative	3.19
SSA_1398	hlyIII/membrane protein, hemolysin III-like, putative	3.88
SSA_1925	serS/seryl-tRNA synthetase, putative	4.41
Down-regulated		
SSA_0068	adhE/alcohol-acetaldehyde dehydrogenase, putative	3.84
SSA_0220	PTS system, mannose-specific IIB component, putative	3.09

and the transgenic complemented strain compared with the *luxS* mutant, indicating a functional complementation of the *luxS* deletion on transcriptional level.

AI-2 Regulates Competence—Next we investigated whether there are genes of *S. sanguinis* specifically regulated by AI-2. The array experiments were repeated by culturing the *S. sanguinis* SR $\Delta luxS/sahH$ strain with and without the addition of DPD. This expression analysis revealed nine differentially expressed genes with a fold change of ≥ 3 ($p \leq 0.05$; Table 3). Among them we identified a putative hemolysin, a putative secreted peptidoglycan hydrolase, and three up-regulated genes coding for competence proteins (*comYA*, *comYB*, and *comGF*). This suggested that the main activity of AI-2 substance could be regulation of competence in *S. sanguinis*. This hypothesis was experimentally challenged and confirmed by testing the natural competence of the *S. sanguinis* WT, its *luxS* mutant, and the heterologous *sahH* complemented *luxS* mutant (Fig. 6). In the absence of external DPD, the transformation efficiency of the *luxS* mutant, as well as of the *sahH* complemented *luxS* mutant, was significantly reduced compared with the WT strain. The addition of DPD resulted in modest enhancement of competence of both strains, but without restoring WT level. These findings underscore the relevance of AI-2 in competence development in *S. sanguinis*.

DISCUSSION

In the present study we addressed the issue of the genome wide consequences of a *luxS* mutation in *S. sanguinis*, its potential effects on oral streptococcal biofilm formation, and which molecular defects lead to the observed phenotype. The latter is difficult to study because deletion of LuxS has three potential consequences: autoinducer-2 substance pools are depleted, methionine produced via the AMC is not available, and finally, the AMC toxic intermediate SAH cannot be degraded (Fig. 1).

We first quantified the AI-2 release in *S. sanguinis* and found maximum release linked to the onset of biofilm formation. This finding did not support a predominant role of LuxS/AI-2 pathways in quorum sensing, a fact also noted for *S. pneumoniae* LuxS mutants by functional experiments (21). In addition, known AI-2 receptors are lacking in many species according to genome sequence analyses (51).

Deletion of LuxS abolished AI-2 substance pool formation, as measured via *V. harveyi* assays. This consequence was noted in all streptococcal species investigated so far (24, 27, 30, 52–54).

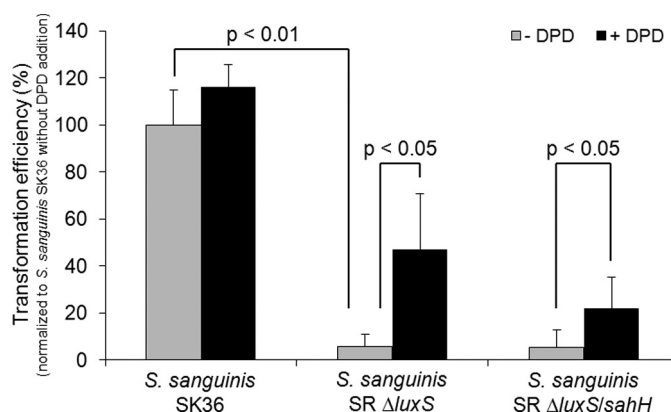


FIGURE 6. **Transformation efficiency assay.** *S. sanguinis* SK36, *S. sanguinis* SR $\Delta luxS$, and *S. sanguinis* SR $\Delta luxS/sahH$ were grown in competence medium with and without the addition of DPD. After reaching A_{600} of ~ 0.2 transforming plasmid DNA was added to the cultures. Contemporaneously, DPD was added for a second time. Transformants and viable cells were numbered by counting colony forming units on BHI agar supplemented with tetracycline and on nonselective agar plates. Transformation efficiency was calculated as a ratio of the number of transformants and total viable cells (47). The values are expressed as percentages of *S. sanguinis* SK36 without the addition of DPD. The error bars indicate standard deviation, and *p* values indicate the corresponding grade of significance.

The *S. sanguinis* LuxS mutant was significantly attenuated in biofilm formation, indicating that the complex consequences of LuxS activity within the AMC are crucial for AI-2 production and biofilm formation in this species. Genetic complementation with a plasmid-encoded autologous *luxS* gene fully restored AI-2 production and biofilm formation over the growth cycle. This was not unexpected and has been shown for many streptococcal species like *S. pneumoniae* and *Streptococcus gordonii* (23, 29).

Synthetic, autologous, and also heterologous AI-2 addition to many of the LuxS mutants has allowed a partial restoration of the phenotype and revealed the quorum sensing contribution of the AMC. For example, *S. mutans* LuxS mutants were successfully complemented by exposure to WT supernatants, supernatants from heterologous species, and also synthetic DPD (25, 26, 31). *S. anginosus*, *Streptococcus suis*, and *S. intermedius* LuxS mutants were also phenotypically restored by AI-2 addition (53–55).

In our study multiple approaches for applying AI-2 and WT supernatants to the *S. sanguinis* LuxS mutant did not restore the defect in biofilm formation. This argues against an AI-2-dependent quorum sensing-mediated control of biofilm forma-

tion in *S. sanguinis* and hints at the influence of other defects caused by the LuxS mutation. One possibility would be a restoration of the metabolic defects of LuxS mutation without affecting the production of AI-2 pool substances. The SahH (EC 3.3.1.1) catalyzes the conversion from SAH to homocysteine in a single step bypassing AI-2 substance pool formation (Fig. 1 and Refs. 5, 9, and 12). From experiments in Gram-negative species, it is known that this pathway can produce sufficient amounts of methionine (15, 16). Expression of SahH in the *S. sanguinis* LuxS mutant restored biofilm development back to WT levels without any detectable AI-2 production (Figs. 2D and 4). This evidence supports the notion of an AI-2-independent biofilm formation in *S. sanguinis*. In addition, this experiment demonstrated that SahH complementation also works in Gram-positive species and thus can serve as a tool for analysis of LuxS-mediated phenotypes in these bacteria as well.

The results described and discussed above lead to the issue of the relevant functions of AI-2 substances in the lifestyle of *S. sanguinis*. The addition of synthetic AI-2 to the SahH-complemented LuxS mutant and investigation of genome-wide expression in all recombinant strains allowed us to address this issue.

In a first series of experiments, we found that the inactivated Pfs/LuxS pathway in *S. sanguinis* influenced genes with central roles in cell growth and metabolism, a fact also observed in other species (9, 12). Of note, the general stress response was induced in the LuxS mutant. This could be due to the accumulation of S-ribosylhomocysteine or SAH caused by the interrupted Pfs/LuxS pathway. SAH is known to be a toxic intermediate (56, 57). In line with these results, the acid stress response was affected in LuxS mutants of *S. mutans*, *S. pyogenes*, and *Lactobacillus spp.*, respectively (19, 25, 58).

In the related species *S. mutans* up to one-third of the whole transcriptome was altered by deletion of LuxS with many similar changes in gene transcript amounts as observed in our study (31). Another global study in *S. mutans* detected 60 genes altered in their transcript abundance (32). This supports a central metabolic role of LuxS and the AMC and leads to the question whether the metabolic changes in the LuxS mutant are due to direct or indirect effects. Apparently, LuxS mutation does not cause growth deficiencies. A rather moderately changed pattern of gene regulation observed in our study could explain this. Alternatively, an additional pathway for methionine production as described in Gram-negative could exist in Gram-positive species. For instance, in *E. coli* homocysteine can be produced via a pathway starting with oxalacetate (16).

SahH complementation in the *S. sanguinis* LuxS mutant background almost completely restored the transcriptional differences induced in the LuxS mutant (209 of 216 genes (97%)). Within the minor fraction of unrestored genes, we identified *purL* and *purB*, coding for a phosphoribosylformylglycinamide synthase and an adenylosuccinate lyase, respectively. These enzymes are involved in purine metabolism (Kyoto Encyclopedia of Genes and Genomes). The differential expression in the WT and the *sahH* complemented strain could be explained by the generation of different byproducts occurring within the Pfs/LuxS and the SahH pathway; the conversion from SAH to homocysteine results in the generation of adenine

or adenosine in the Pfs/LuxS pathway or SahH reaction, respectively (Fig. 1 and Refs. 5 and 12). This may cause an altered regulation of genes and enzymes involved in purine metabolism and thus could explain the altered transcription of *purL* and *purB*. Five more genes were not restored by the expression of *sahH*: *clpL*, *ctpA*, and three genes of unknown function (SSA 0141, SSA 1354, and SSA 2276). SSA 0141 encodes for a putative copper chaperone and belongs to the same operon as *ctpA*, a copper translocating P-type ATPase (Kyoto Encyclopedia of Genes and Genomes). ClpL is a chaperone not involved in protein degradation, because of the missing recognition tripeptide, which enables the interaction with ClpP (59). It is involved in stress tolerance and biofilm formation (60, 61).

Altogether, the expression of *sahH* restored the effects of the *luxS* deletion on transcriptome level except a minor fraction of genes. This should be considered in future studies of *luxS* mutants.

In a second series of experiments, the addition of AI-2 substance to a culture of the *S. sanguinis* LuxS mutant complemented with *sahH* uncovered the direct AI-2-dependent responsive network. Of note, only a small number of genes responded to this treatment. Mainly genes involved in genetic competence development are dependent on the presence of the AMC byproduct AI-2, in particular those involved in DNA binding and uptake. The transformation efficiency assay confirmed the prediction of reduced competence in the *luxS* mutant, as well as in the *sahH*-complemented strain. As expected, the addition of DPD elevated the level of competence in the *luxS* strain but surprisingly also demonstrated a measurable effect in the *sahH*-complemented strain. This suggests a level of complexity in which the defect within the AMC caused by missing LuxS activity in the *luxS* mutant also has a negative effect on competence over and above AMC-independent effects on competence that stem directly from the lack of AI-2. A further confounding factor may be copy number effects of the gene coding for SahH, which is located on a high copy number plasmid and which could have interfered with the transforming plasmid DNA. *S. sanguinis* WT and the *luxS* mutant did not possess any plasmid.

The deletion of *luxS* has a negative effect on natural competence. This has been demonstrated for *S. mutans* and is consistent with the findings of the present study (47). An influence on expression of late competence genes was also found in LuxS mutants of *S. pneumoniae* (22, 62); however, in those studies the direct influence of AI-2 was not investigated.

S. sanguinis is naturally competent, a feature that is controlled by stress response pathways and competence-stimulating peptides (63–65). Our data also suggest that also AI-2 substance potentially has an influence on natural competence of this species.

In summary we have shown that (i) *S. sanguinis* biofilm formation is independent of AI-2 based quorum sensing; (ii) genetic complementation of LuxS mutants with autologous or heterologous genes, as well as chemical complementation with AI-2 substances, is not sufficient to determine the exact biological roles of the AMC components; (iii) a heterologous complementation with SahH as a pathway short cut restored the metabolic deficiencies of LuxS mutation; and (iv) such a com-

plemented strain in combination with chemical complementation could be the tool of choice to determine the individual biological roles of AI-2-based quorum sensing and AMC metabolic functions. Based on the results presented here, also *LuxS* mutants in other Gram-positive species might be subjected to a second look at their methionine pool and AI-2-dependent pathways.

Acknowledgments—We thank G. Fulda and W. Labs from the Electron Microscopic Centre of the Medical Faculty of the University of Rostock for technical assistance.

REFERENCES

- Greenberg, E. P., Hastings, J. W., and Ulitzur, S. (1979) Induction of luciferase synthesis in *Benekeia harveyi* by other marine bacteria. *Arch. Microbiol.* **120**, 87–91
- Bassler, B. L., Wright, M., and Silverman, M. R. (1994) Multiple signalling systems controlling expression of luminescence in *Vibrio harveyi*. Sequence and function of genes encoding a second sensory pathway. *Mol. Microbiol.* **13**, 273–286
- Bassler, B. L., Greenberg, E. P., and Stevens, A. M. (1997) Cross-species induction of luminescence in the quorum-sensing bacterium *Vibrio harveyi*. *J. Bacteriol.* **179**, 4043–4045
- Xavier, K. B., and Bassler, B. L. (2005) Interference with AI-2-mediated bacterial cell-cell communication. *Nature* **437**, 750–753
- Sun, J., Daniel, R., Wagner-Döbler, I., and Zeng, A. P. (2004) Is autoinducer-2 a universal signal for interspecies communication. A comparative genomic and phylogenetic analysis of the synthesis and signal transduction pathways. *BMC Evol. Biol.* **4**, 36
- Surette, M. G., Miller, M. B., and Bassler, B. L. (1999) Quorum sensing in *Escherichia coli*, *Salmonella typhimurium*, and *Vibrio harveyi*. A new family of genes responsible for autoinducer production. *Proc. Natl. Acad. Sci. U.S.A.* **96**, 1639–1644
- McNab, R., and Lamont, R. J. (2003) Microbial dinner-party conversations. The role of *LuxS* in interspecies communication. *J. Med. Microbiol.* **52**, 541–545
- Rickard, A. H., Palmer, R. J., Jr., Blehert, D. S., Campagna, S. R., Semmelhack, M. F., Eglund, P. G., Bassler, B. L., and Kolenbrander, P. E. (2006) Autoinducer 2. A concentration-dependent signal for mutualistic bacterial biofilm growth. *Mol. Microbiol.* **60**, 1446–1456
- Vendeville, A., Winzer, K., Heurlier, K., Tang, C. M., and Hardie, K. R. (2005) Making 'sense' of metabolism. Autoinducer-2, *LuxS* and pathogenic bacteria. *Nat. Rev. Microbiol.* **3**, 383–396
- Hardie, K. R., and Heurlier, K. (2008) Establishing bacterial communities by 'word of mouth.' *LuxS* and autoinducer 2 in biofilm development. *Nat. Rev. Microbiol.* **6**, 635–643
- Antunes, L. C., Ferreira, R. B., Buckner, M. M., and Finlay, B. B. (2010) Quorum sensing in bacterial virulence. *Microbiology* **156**, 2271–2282
- Parveen, N., and Cornell, K. A. (2011) Methylthioadenosine/S-adenosylhomocysteine nucleosidase, a critical enzyme for bacterial metabolism. *Mol. Microbiol.* **79**, 7–20
- Winzer, K., Hardie, K. R., Burgess, N., Doherty, N., Kirke, D., Holden, M. T., Linforth, R., Cornell, K. A., Taylor, A. J., Hill, P. J., and Williams, P. (2002) *LuxS*. Its role in central metabolism and the in vitro synthesis of 4-hydroxy-5-methyl-3(2H)-furanone. *Microbiology* **148**, 909–922
- Schauder, S., Shokat, K., Surette, M. G., and Bassler, B. L. (2001) The *LuxS* family of bacterial autoinducers. Biosynthesis of a novel quorum-sensing signal molecule. *Mol. Microbiol.* **41**, 463–476
- Shao, H., Lamont, R. J., and Demuth, D. R. (2007) Autoinducer 2 is required for biofilm growth of *Aggregatibacter (Actinobacillus) actinomycetemcomitans*. *Infect. Immun.* **75**, 4211–4218
- Walters, M., Sircili, M. P., and Sperandio, V. (2006) AI-3 synthesis is not dependent on *luxS* in *Escherichia coli*. *J. Bacteriol.* **188**, 5668–5681
- Lyon, W. R., Madden, J. C., Levin, J. C., Stein, J. L., and Caparon, M. G. (2001) Mutation of *luxS* affects growth and virulence factor expression in *Streptococcus pyogenes*. *Mol. Microbiol.* **42**, 145–157
- Marouni, M. J., and Sela, S. (2003) The *luxS* gene of *Streptococcus pyogenes* regulates expression of genes that affect internalization by epithelial cells. *Infect. Immun.* **71**, 5633–5639
- Siller, M., Janapatla, R. P., Pirzada, Z. A., Hassler, C., Zinkl, D., and Charpentier, E. (2008) Functional analysis of the group A streptococcal *luxS*/AI-2 system in metabolism, adaptation to stress and interaction with host cells. *BMC Microbiol.* **8**, 188
- Stroeher, U. H., Paton, A. W., Ogunniyi, A. D., and Paton, J. C. (2003) Mutation of *luxS* of *Streptococcus pneumoniae* affects virulence in a mouse model. *Infect. Immun.* **71**, 3206–3212
- Joyce, E. A., Kawale, A., Censini, S., Kim, C. C., Covacci, A., and Falkow, S. (2004) *LuxS* is required for persistent pneumococcal carriage and expression of virulence and biosynthesis genes. *Infect. Immun.* **72**, 2964–2975
- Romao, S., Memmi, G., Oggioni, M. R., and Trombe, M. C. (2006) *LuxS* impacts on LytA-dependent autolysis and on competence in *Streptococcus pneumoniae*. *Microbiology* **152**, 333–341
- Vidal, J. E., Ludewick, H. P., Kunkel, R. M., Zähler, D., and Klugman, K. P. (2011) The *LuxS*-dependent quorum-sensing system regulates early biofilm formation by *Streptococcus pneumoniae* strain D39. *Infect. Immun.* **79**, 4050–4060
- Merritt, J., Qi, F., Goodman, S. D., Anderson, M. H., and Shi, W. (2003) Mutation of *luxS* affects biofilm formation in *Streptococcus mutans*. *Infect. Immun.* **71**, 1972–1979
- Wen, Z. T., and Burne, R. A. (2004) *LuxS*-mediated signaling in *Streptococcus mutans* is involved in regulation of acid and oxidative stress tolerance and biofilm formation. *J. Bacteriol.* **186**, 2682–2691
- Yoshida, A., Ansai, T., Takehara, T., and Kuramitsu, H. K. (2005) *LuxS*-based signaling affects *Streptococcus mutans* biofilm formation. *Appl. Environ. Microbiol.* **71**, 2372–2380
- Petersen, F. C., Ahmed, N. A., Naemi, A., and Scheie, A. A. (2006) *LuxS*-mediated signalling in *Streptococcus anginosus* and its role in biofilm formation. *Antonie Van Leeuwenhoek* **90**, 109–121
- Blehert, D. S., Palmer, R. J., Jr., Xavier, J. B., Almeida, J. S., and Kolenbrander, P. E. (2003) Autoinducer 2 production by *Streptococcus gordonii* DL1 and the biofilm phenotype of a *luxS* mutant are influenced by nutritional conditions. *J. Bacteriol.* **185**, 4851–4860
- McNab, R., Ford, S. K., El-Sabaeny, A., Barbieri, B., Cook, G. S., and Lamont, R. J. (2003) *LuxS*-based signaling in *Streptococcus gordonii*. Autoinducer 2 controls carbohydrate metabolism and biofilm formation with *Porphyromonas gingivalis*. *J. Bacteriol.* **185**, 274–284
- Ahmed, N. A., Petersen, F. C., and Scheie, A. A. (2008) Biofilm formation and autoinducer-2 signaling in *Streptococcus intermedius*. Role of thermal and pH factors. *Oral Microbiol. Immunol.* **23**, 492–497
- Sztajer, H., Lemme, A., Vilchez, R., Schulz, S., Geffers, R., Yip, C. Y., Levesque, C. M., Cvitkovitch, D. G., and Wagner-Döbler, I. (2008) Autoinducer-2-regulated genes in *Streptococcus mutans* UA159 and global metabolic effect of the *luxS* mutation. *J. Bacteriol.* **190**, 401–415
- Wen, Z. T., Nguyen, A. H., Bitoun, J. P., Abranches, J., Baker, H. V., and Burne, R. A. (2011) Transcriptome analysis of *LuxS*-deficient *Streptococcus mutans* grown in biofilms. *Mol. Oral Microbiol.* **26**, 2–18
- Dyson, C., Barnes, R. A., and Harrison, G. A. (1999) Infective endocarditis. An epidemiological review of 128 episodes. *J. Infect.* **38**, 87–93
- Mylonakis, E., and Calderwood, S. B. (2001) Infective endocarditis in adults. *N. Engl. J. Med.* **345**, 1318–1330
- Facklam, R. (2002) What happened to the streptococci. Overview of taxonomic and nomenclature changes. *Clin. Microbiol. Rev.* **15**, 613–630
- Bertani, G. (1951) Studies on lysogeny. I. The mode of phage liberation by lysogenic *Escherichia coli*. *J. Bacteriol.* **62**, 293–300
- Bertani, G. (2004) Lysogeny at mid-twentieth century. P1, P2, and other experimental systems. *J. Bacteriol.* **186**, 595–600
- van de Rijn, I., and Kessler, R. E. (1980) Growth characteristics of group A streptococci in a new chemically defined medium. *Infect. Immun.* **27**, 444–448
- Standar, K., Kreikemeyer, B., Redanz, S., Münster, W. L., Laue, M., and Podbielski, A. (2010) Setup of an *in vitro* test system for basic studies on biofilm behavior of mixed-species cultures with dental and periodontal pathogens. *PLoS One* **5**, e13135

40. Kushner, S. R. (1978) An improved method for transformation of *Escherichia coli* with *col* El-derived plasmids. *Genetic Engineering* 17–23
41. Grinwis, M. E., Sibley, C. D., Parkins, M. D., Eshaghurshan, C. S., Rabin, H. R., and Surette, M. G. (2010) Characterization of *Streptococcus milleri* group isolates from expectorated sputum of adult patients with cystic fibrosis. *J. Clin. Microbiol.* **48**, 395–401
42. Mok, K. C., Wingreen, N. S., and Bassler, B. L. (2003) *Vibrio harveyi* quorum sensing. A coincidence detector for two autoinducers controls gene expression. *EMBO J.* **22**, 870–881
43. Redanz, S., Standar, K., Podbielski, A., and Kreikemeyer, B. (2011) A five-species transcriptome array for oral mixed-biofilm studies. *PLoS One* **6**, e27827
44. Irizarry, R. A., Hobbs, B., Collin, F., Beazer-Barclay, Y. D., Antonellis, K. J., Scherf, U., and Speed, T. P. (2003) Exploration, normalization, and summaries of high density oligonucleotide array probe level data. *Biostatistics*. **4**, 249–264
45. Shaw, R. G., and Mitchell-Olds, T. (1993) ANOVA for unbalanced data. An overview. *Ecology* **74**, 1638–1645
46. Benjamini, Y., and Hochberg, Y. (1995) Controlling the false discovery rate: A practical and powerful approach to multiple testing. *J. R. Stat. Soc. B* **57**, 289–300
47. Merritt, J., Qi, F., and Shi, W. (2005) A unique nine-gene comY operon in *Streptococcus mutans*. *Microbiology* **151**, 157–166
48. Podbielski, A., Spellerberg, B., Woischnik, M., Pohl, B., and Lütticken, R. (1996) Novel series of plasmid vectors for gene inactivation and expression analysis in group A streptococci (GAS). *Gene* **177**, 137–147
49. McNab, R. (2003) LuxS-based signaling in *Streptococcus gordonii*. Auto-inducer 2 controls carbohydrate metabolism and biofilm formation with *Porphyromonas gingivalis*. *J. Bacteriol.* **185**, 274–284
50. De Keersmaecker, S. C., Varszegi, C., van Boxel, N., Habel, L. W., Metzger, K., Daniels, R., Marchal, K., De Vos, D., and Vanderleyden, J. (2005) Chemical synthesis of (S)-4,5-dihydroxy-2,3-pentanedione, a bacterial signal molecule precursor, and validation of its activity in *Salmonella typhimurium*. *J. Biol. Chem.* **280**, 19563–19568
51. Rezzonico, F., and Duffy, B. (2008) Lack of genomic evidence of AI-2 receptors suggests a non-quorum sensing role for luxS in most bacteria. *BMC Microbiol.* **8**, 154
52. Cao, M., Feng, Y., Wang, C., Zheng, F., Li, M., Liao, H., Mao, Y., Pan, X., Wang, J., Hu, D., Hu, F., and Tang, J. (2011) Functional definition of LuxS, an autoinducer-2 (AI-2) synthase and its role in full virulence of *Streptococcus suis* serotype 2. *J. Microbiol.* **49**, 1000–1011
53. Pecharki, D., Petersen, F. C., and Scheie, A. A. (2008) LuxS and expression of virulence factors in *Streptococcus intermedius*. *Oral Microbiol. Immunol.* **23**, 79–83
54. Wang, Y., Zhang, W., Wu, Z., Zhu, X., and Lu, C. (2011) Functional analysis of luxS in *Streptococcus suis* reveals a key role in biofilm formation and virulence. *Vet. Microbiol.* **152**, 151–160
55. Ahmed, N. A., Petersen, F. C., and Scheie, A. A. (2007) AI-2 quorum sensing affects antibiotic susceptibility in *Streptococcus anginosus*. *J. Antimicrob. Chemother.* **60**, 49–53
56. Ueland, P. M. (1982) Pharmacological and biochemical aspects of S-adenosylhomocysteine and S-adenosylhomocysteine hydrolase. *Pharmacol. Rev.* **34**, 223–253
57. Christopher, S. A., Melnyk, S., James, S. J., and Kruger, W. D. (2002) S-Adenosylhomocysteine, but not homocysteine, is toxic to yeast lacking cystathionine β -synthase. *Mol. Genet. Metab* **75**, 335–343
58. Moslehi-Jenabian, S., Gori, K., and Jespersen, L. (2009) AI-2 signalling is induced by acidic shock in probiotic strains of *Lactobacillus* spp. *Int. J. Food Microbiol.* **135**, 295–302
59. Kim, Y. I., Levchenko, I., Fraczowska, K., Woodruff, R. V., Sauer, R. T., and Baker, T. A. (2001) Molecular determinants of complex formation between Clp/Hsp100 ATPases and the ClpP peptidase. *Nat. Struct. Biol.* **8**, 230–233
60. Kajfasz, J. K., Martinez, A. R., Rivera-Ramos, I., Abranches, J., Koo, H., Quivey, R. G., Jr., and Lemos, J. A. (2009) Role of Clp proteins in expression of virulence properties of *Streptococcus mutans*. *J. Bacteriol.* **191**, 2060–2068
61. Kwon, H. Y., Kim, S. W., Choi, M. H., Ogunniyi, A. D., Paton, J. C., Park, S. H., Pyo, S. N., and Rhee, D. K. (2003) Effect of heat shock and mutations in ClpL and ClpP on virulence gene expression in *Streptococcus pneumoniae*. *Infect. Immun.* **71**, 3757–3765
62. Trappetti, C., Potter, A. J., Paton, A. W., Oggioni, M. R., and Paton, J. C. (2011) LuxS mediates iron-dependent biofilm formation, competence, and fratricide in *Streptococcus pneumoniae*. *Infect. Immun.* **79**, 4550–4558
63. Callahan, J. E., Munro, C. L., and Kitten, T. (2011) The *Streptococcus sanguinis* competence regulon is not required for infective endocarditis virulence in a rabbit model. *PLoS One* **6**, e26403
64. Rodriguez, A. M., Callahan, J. E., Fawcett, P., Ge, X., Xu, P., and Kitten, T. (2011) Physiological and molecular characterization of genetic competence in *Streptococcus sanguinis*. *Mol. Oral Microbiol.* **26**, 99–116
65. Zhu, L., Zhang, Y., Fan, J., Herzberg, M. C., and Kreth, J. (2011) Characterization of competence and biofilm development of a *Streptococcus sanguinis* endocarditis isolate. *Mol. Oral Microbiol.* **26**, 117–126
66. Chen, X. (2002) Structural identification of a bacterial quorum-sensing signal containing boron. *Nature* **415**, 545–549
67. Miller, S. T. (2004) *Salmonella typhimurium* recognizes a chemically distinct form of the bacterial quorum-sensing signal AI-2. *Mol. Cell* **15**, 677–687
68. Hanahan, D. (1983) Studies on transformation of *Escherichia coli* with plasmids. *J. Mol. Biol.* **166**, 557–580
69. Trieu-Cuot, P., Carlier, C., Poyart-Salmeron, C., and Courvalin, P. (1991) Shuttle vectors containing a multiple cloning site and a lacZ α gene for conjugal transfer of DNA from *Escherichia coli* to gram-positive bacteria. *Gene* **102**, 99–104
70. Short, J. M., Fernandez, J. M., Sorge, J. A., and Huse, W. D. (1988) Lambda ZAP. A bacteriophage lambda expression vector with in vivo excision properties. *Nucleic Acids Res.* **16**, 7583–7600
71. Biswas, I., Jha, J. K., and Fromm, N. (2008) Shuttle expression plasmids for genetic studies in *Streptococcus mutans*. *Microbiology* **154**, 2275–2282
72. Yanisch-Perron, C., Vieira, J., and Messing, J. (1985) Improved M13 phage cloning vectors and host strains. Nucleotide sequences of the M13mp18 and pUC19 vectors. *Gene* **33**, 103–119